Is multileaf collimator tracking or gating a better intrafraction motion adaptation strategy? An analysis of the TROG 15.01 Stereotactic Prostate Ablative Radiotherapy with KIM (SPARK) trial

Emily A Hewson[1*], Doan Trang Nguyen[1,2], Ricky O'Brien[1], Per R Poulsen[3], Jeremy T Booth[4,5], Peter Greer[6], Thomas Eade[4], Andrew Kneebone[4], George Hruby[4], Trevor Moodie[7], Amy J Hayden[7], Sandra L Turner[7], Nicholas Hardcastle[8], Shankar Siva[8], Keen Hun Tai[8], Jarad Martin[6] and Paul J Keall[1]

[1]*ACRF Image X Institute, University of Sydney Medical School, Sydney, Australia,* [2]*School of Biomedical Engineering, University of Technology Sydney, Ultimo, Sydney, Australia*

[3]*Department of Oncology, Aarhus University Hospital, Aarhus, Denmark,* [4]*Northern Sydney Cancer Centre, Royal North Shore Hospital, Sydney, Australia,* [5]*School of Physics, University of Sydney, Sydney, Australia,* [6]*Calvary Mater Newcastle, Waratah, Australia*

[7]*Crown Princess Mary Cancer Centre, Westmead, Sydney, Australia,* [8]*Peter MacCallum Cancer Centre, Melbourne, Australia,*

[*]Corresponding author at: University of Sydney, Sydney, Australia

E-mail address: emily.hewson@sydney.edu.au

Postal address:
The University of Sydney
Camperdown NSW 2006

Abstract

Purpose: Stereotactic Ablative Radiotherapy (SABR) has recently emerged as a favourable treatment option for prostate cancer patients. With higher doses delivered over fewer fractions, motion adaptation is a requirement for accurate delivery of SABR. This study compared the efficacy of multileaf collimator (MLC) tracking vs. gating as a real-time motion adaptation strategy for prostate cancer SABR patients enrolled in a clinical trial.

Methods: Forty-four prostate patients treated over five fractions in the TROG 15.01 SPARK trial were analysed in this study. Forty-nine fractions were treated using MLC tracking and 166 fractions were treated using beam gating and couch shifts. A time-resolved motion-encoded dose reconstruction method was used to evaluate the dose delivered using each motion adaptation strategy and compared to an estimation of what would have been delivered with no motion adaptation strategy implemented.

Results: MLC tracking and gating both delivered doses closer to the plan compared to when no motion adaptation strategy was used. Differences between MLC tracking and gating were small with differences in the mean discrepancy from the plan of -0.3% (CTV $D_{98\%}$), 1.4% (CTV $D_{2\%}$), 0.4% (PTV $D_{95\%}$), 0.2% (rectum V_{30Gy}) and 0.0% (bladder V_{30Gy}). On average, 0.5 couch shifts were required per gated fractions with a mean interruption duration of 1.8 ± 2.6 minutes per fraction treated using gating.

Conclusion: Both MLC tracking and gating were effective strategies at improving the accuracy of the dose delivered to the target and organs at risk. While dosimetric performance was comparable, gating resulted in interruptions to treatment.

Clinical trial registration number: NCT02397317

Introduction

Stereotactic ablative radiotherapy (SABR) has recently shown promising potential for the treatment of prostate cancer [1-5] with support for the use of SABR for low and intermediate risk patients [6], and the number of clinics opting to use SABR to treat patients is increasing [7]. However, due to the escalated biological effect and requirement for stricter treatment margins, techniques to manage intrafraction tumour motion must be implemented to achieve safe and accurate SABR [8, 9].

To allow for accurate treatment delivery, dedicated systems have been developed to adapt to intrafraction motion. The CyberKnife robotic adaptation system (Accuray Inc, Sunnyvale, USA) [10], the Radixact system (Accuray Inc, Sunnyvale, USA) [11], and the Vero gimballed adaptation system (Brainlab, Munich, Germany) [12] are examples of commercial systems that were designed to perform real-time tumour tracking, but as they involve highly specialised technology and high costs, the adoption in clinics has been limited.

It would be preferable to perform real-time tumour motion adaptation on a standard linear accelerator (linac). Gating the treatment beam can be performed on standard linacs for improving treatment accuracy. Gating is one of the most widely used techniques for managing motion during the treatment of tumours affected by respiratory motion [13]. Gating can also be used to correct for genitourinary and gastrointestinal motion in combination with couch shifts to realign the patient to the planned position, and has been used to treat prostate cancer patients [14, 15]. More recently, multileaf collimator (MLC) tracking has been developed and clinically implemented [16], providing a solution for real-time intrafraction motion adaptation that can also be implemented on a standard linac. MLC tracking has been used to treat prostate cancer patients during standard fractionation [17] and SABR [18] treatments as well as for lung cancer patients [19].

MLC tracking and gating were both used for intrafraction motion adaptation during prostate SABR treatments in the Trans-Tasman Radiation Oncology Group (TROG) 15.01 Stereotactic Prostate Ablative Radiotherapy with KIM (SPARK) clinical trial [20]. The primary aim of the TROG 15.01 SPARK trial was to quantify the delivered dose using KIM intervention to test improvements in patient dose distributions, cancer targeting accuracy, and patient outcomes compared to treatment without KIM intervention. The aim of this study was to compare the doses delivered using MLC tracking and gating for the cohort of patients treated using SABR in the TROG 15.01 SPARK trial.

Materials and Methods

Clinical trial details

The TROG 15.01 SPARK trial (NCT02397317) treated 48 prostate cancer patients with low to intermediate risk using SABR at five treatment centres. The trial protocol was approved by the Hunter New England Human Research Ethics Committee and all patients provided informed written consent. Patients were prescribed a dose of 36.25 Gy to 95% of the planning target volume (PTV) in five fractions. The PTV included a 5 mm expansion from the clinical target volume (CTV) in each direction, except posteriorly which had a 3 mm expansion. Treatment was delivered using volumetric modulated arc therapy (VMAT) on either a Varian Trilogy, Varian TrueBeam (Varian Medical Systems, Palo Alto, USA), or an Elekta Synergy linac (Elekta, Crawley, UK). The trial protocol and dose-volume constraints were described in detail by Keall, *et. al* [20]. All patients were implanted with three gold fiducial markers to enable image guidance.

Motion adaptation process

Motion guidance was performed using Kilovoltage Intrafraction Monitoring (KIM) which used the on-board kV imager to acquire images of the patient during treatment at 10 frames per second. KIM automatically segmented the fiducial markers implanted in the prostate and

from these 2D projections, estimated the 3D position [21] as well as rotation [22]. The geometric accuracy and precision of KIM implemented in the 15.01 SPARK trial was found to be within 0.5 mm for translation and 1.4° for rotation [23].

Intrafraction KIM-guided motion adaptation was then performed by either MLC tracking or gating. Both methods corrected for 3D translational motion. Intrafraction prostate rotation was not corrected in this study. MLC tracking corrected for motion in real-time by recalculating the optimal leaf positions based on the leaf positions from the treatment plan and the new target position such that underexposure and overexposure were minimised [16]. MLC tracking was implemented for 10 patients treated at one of the four treatment centres using a Millennium 120-leaf MLC on the Varian Trilogy, with the exception of one fraction that was treated using gating, for a total of 49 fractions.

Gating was performed at the remaining three Varian treatment centres and intervention was performed when the prostate's motion exceeded 2 mm (29 patients) or 3 mm (5 patients) for longer than 5 seconds in any direction, or immediately if motion exceeded 5 mm. The 3 mm threshold was predetermined in the trial protocol due to the PTV margin of 3 mm in the posterior direction, and stricter thresholds of 2 mm were used at the institutions' discretion. Once the treatment beam was manually gated, the couch was shifted to reposition the patient such that the prostate was returned to its initial planned position. Gating was available for 171 fractions, but treatment was not completed using KIM for 5 fractions due to various technical issues [24]. A total of 166 gating fractions were included in this analysis, and 65 of these fractions observed prostate motion that exceeded the motion threshold, requiring intervention.

The latency of KIM was previously measured to be within 350 ms, and the latency of MLC tracking was 230 ± 20 ms [16]. The total system latency is under 1 s and is

considerably smaller than the 5 second gating threshold. The MLC tracking latency is not expected to have a significant dosimetric impact for prostate treatments due to the slow movement of the prostate. To ensure that MLC tracking did not have a negative dosimetric impact, each patient plan that was treated using MLC tracking underwent pre-treatment quality assurance, described previously by Keall et al. [18]. Delivered dose with MLC tracking to a phantom placed on a motion platform was measured and compared to the dose delivered without motion. Each of the ten patient plans passed the tolerance of 98% of points within 2%/2 mm using a gamma comparison.

Data analysis

Delivered dose using each adaptation strategy was assessed using a dose reconstruction method previously described by Poulsen, *et. al* [25]. Prostate motion was incorporated into the treatment plan by dividing each treatment arc into several sub-arcs that each had a shifted isocentre that corresponded to the motion trace divided into 1 mm position bins. This time-resolved dose reconstruction method was not able to be performed for the four patients treated with the Elekta synergy linac in this trial, thus a total of 44 patients from four treatment centres were included in the final analysis. From these patient treatments, 215 fractions were completed and analysed in this study.

To calculate the dose delivered during the gating fractions, the prostate motion trace, including couch corrections if any occurred, was encoded into the plan. To calculate the dose delivered during MLC tracking, the updated MLC positions were collected from the DynaLog files at each treatment and included in the reconstructed plan in addition to the measured motion. The dose that would have been delivered if no motion adaptation strategy were used was also estimated for each fraction by encoding the prostate motion that would have occurred without gating or tracking. This workflow is depicted in Figure 1. All doses

were calculated using the planning CT and this dose reconstruction method did not consider rotations or interfraction changes in anatomy.

The delivered dose to two targets, the CTV ($D_{98\%}$ and $D_{2\%}$) and PTV ($D_{95\%}$), and two normal tissues, the rectum and bladder (V_{30Gy}) was considered. The CTV and PTV were both included as the CTV dose is the structure of interest, however, has uncertainties that require the margins creating the PTV. The rectum and bladder were chosen as these are two critical dose-limiting organs for prostate cancer SABR. The total dose delivered for each patient was also assessed by summing the dose across five fractions. The mean differences in dose from the plan were compared using an unpaired t-test and the variances were compared using an F-test. The correlation between prostate motion and differences in dose from the plan were evaluated by calculating a Pearson correlation coefficient (ρ).

The efficiency of gated treatments was evaluated by calculating the time required to gate and perform a couch shift for each fraction. This was calculated by determining the duration of time between the treatment beam being gated off until the treatment beam was switched back on resuming the treatment.

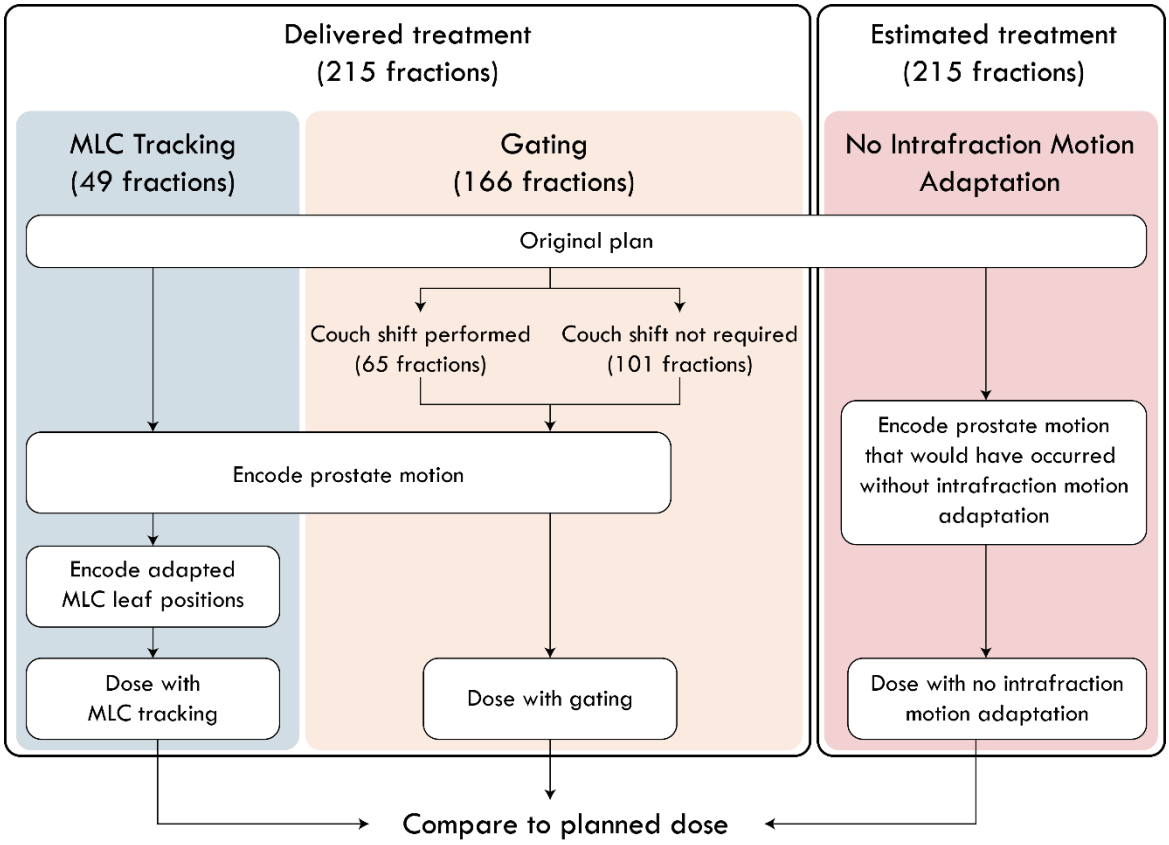

Figure 1. The workflow used to reconstruct the doses delivered during treatment using MLC tracking and gating. The dose that would have been delivered if no intrafraction motion adaptation strategy was implemented was also calculated for each fraction.

Results

The distributions of prostate motion measured during MLC tracking and gating fractions are shown in Figure 2. The means and standard deviations of motion observed for patients treated using MLC tracking were -1.2 ± 2.4 mm (range -9.1 to 10.5 mm), 0.2 ± 1.2 mm (range -3.6 to 3.8 mm) and -1.1 ± 1.8 mm (range -16.9 to 7.6 mm) in the anterior-posterior (AP), left-right (LR) and superior-inferior (SI) directions respectively. The mean and standard deviations of motion observed for patients treated using gating were -0.5 ± 1.6 mm (range -6.2 to 7.5 mm), 0.1 ± 1.0 mm (range -5.9 to 6.0 mm) and -0.6 ± 1.7 mm (range -9.9 to 9.3 mm) in the AP, LR and SI directions respectively.

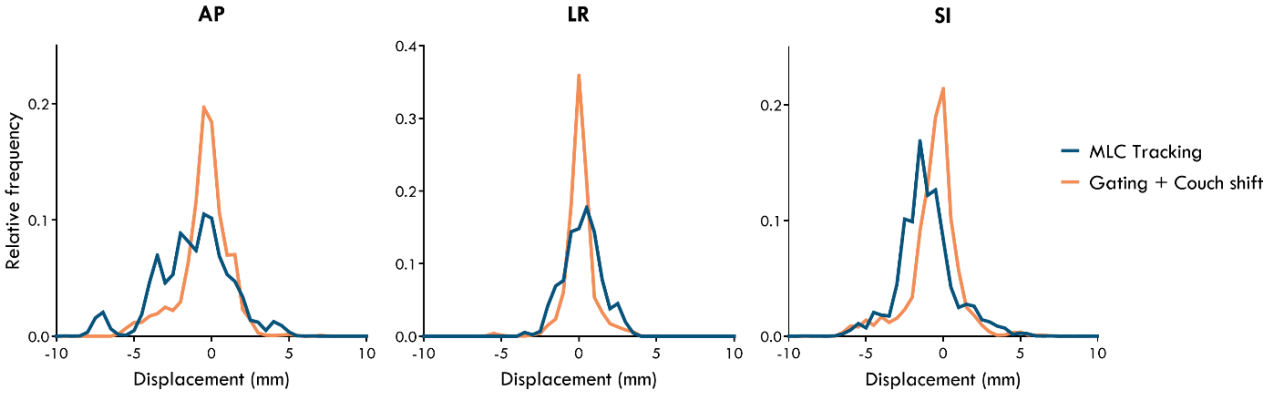

Figure 2. Prostate motion observed in the anterior-posterior, left-right and superior-inferior directions during treatment.

The differences between the planned doses and the doses delivered using MLC tracking and gating, and the doses that would have been delivered without motion adaptation for each fraction, are plotted in Figure 3. The differences of the mean difference from the plan between MLC tracking and gating were -0.3% for the CTV $D_{98\%}$ ($p < 0.05$), 1.4% for the CTV $D_{2\%}$ ($p < 0.05$), 0.4% for the PTV $D_{95\%}$ ($p < 0.05$), 0.2% for the rectum V_{30Gy} ($p < 0.05$) and 0.0% for the bladder V_{30Gy} ($p > 0.05$).

MLC tracking maintained the CTV $D_{98\%}$, CTV $D_{2\%}$ and PTV $D_{95\%}$ to within 3.3%, 4.9% and 2.3% of the plan respectively across all fractions. Gating maintained the CTV $D_{98\%}$, CTV $D_{2\%}$ and PTV $D_{95\%}$ to within 4.6%, 5.3% and 5.2% of the plan respectively. For the organs at risk (OARs), MLC tracking maintained the rectum V_{30Gy} and bladder V_{30Gy} to within 2.5% and 2.3% of the plan, while gating maintained the bladder and rectum doses to within 4.3% and 3.4% of the plan. The variances of the dose differences from the plan for MLC tracking and gating were not significantly different for the CTV $D_{98\%}$, CTV $D_{2\%}$ and PTV $D_{95\%}$ ($p > 0.05$), but gating had significantly larger variances of differences from the plan compared to MLC tracking for the rectum V_{30Gy} and bladder V_{30Gy} ($p < 0.01$).

Similar results are seen when the dose is summed across the entire treatment course of five fractions, however differences from the plan are reduced when considering the whole course for each treatment strategy (Figure 4). The dose differences from the original plan for each patient has been included in the supplementary data. Even when considering the summed dose across five fractions, the treatment that would have been delivered without any intrafraction motion adaptation would have resulted in underdosing to the CTV $D_{98\%}$ and PTV $D_{95\%}$ of up to -5.6% and -17.0% respectively, and overdosing to the rectum V_{30Gy} and bladder V_{30Gy} of up to 1.2% and 8.5% respectively. MLC tracking and gating did not have significantly different mean deviations from the plan ($p > 0.05$) for the summed treatments. However, gating still had a larger variance of differences from the plan than MLC tracking for the bladder ($p < 0.01$).

When no motion adaptation strategy was used, moderate to high correlations between the root-mean-square-error (RMSE) of the 3D prostate displacement and the absolute difference from the plan for the CTV $D_{98\%}$ ($\rho = 0.66$), CTV $D_{2\%}$ ($\rho = 0.46$), PTV $D_{95\%}$ ($\rho = 0.86$), rectum V_{30Gy} ($\rho = 0.65$) and bladder V_{30Gy} ($\rho = 0.72$) were observed ($p < 0.05$). No statistically significant correlation was found between the RMSE of the prostate displacement and any of these dose metrics for MLC tracking ($\rho < 0.16$, $p > 0.05$). The correlations between the RMSE of the prostate displacement and the absolute dose differences from the plan were higher for gating compared to MLC tracking for the CTV $D_{98\%}$ ($\rho = 0.25$), CTV $D_{2\%}$ ($\rho = 0.22$), PTV $D_{95\%}$ ($\rho = 0.32$), and bladder V_{30Gy} ($\rho = 0.32$). The rectum V_{30Gy} had no correlation for gating ($p > 0.05$), comparable to MLC tracking in this study.

The performance of the two motion adaptation strategies with respect to the magnitude of prostate motion that occurred during each fraction is shown in Figure 5. Fractions were categorised as having small prostate motion if the prostate motion did not exceed the threshold that would trigger a gating event (116 fractions), and fractions which

had motion larger than this threshold was categorised a large prostate motion (99 of fractions). The mean differences from the plan for the CTV $D_{98\%}$ was higher for MLC tracking compared to gating ($p < 0.05$) for small motion, but not for large motion. The mean difference from the plan for the CTV $D_{2\%}$ was higher for MLC tracking for both smaller and larger motion fractions ($p > 0.05$). The variance of differences from the plan for the rectum V_{30Gy} and bladder V_{30Gy} was smaller for MLC tracking for both small and large motions ($p < 0.5$).

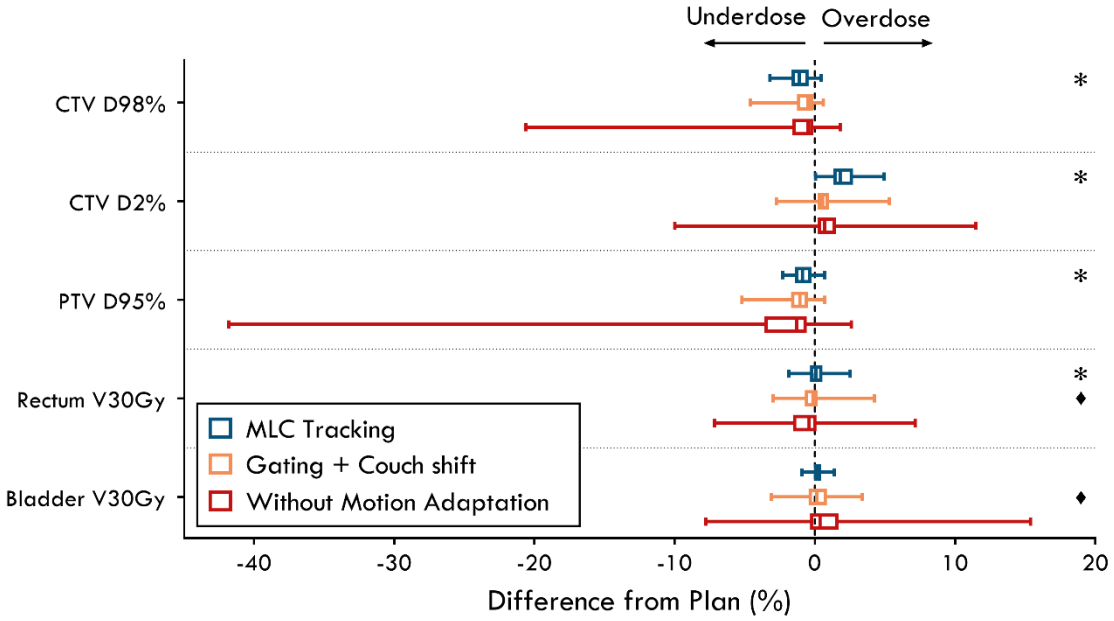

Figure 3. Fraction doses. The differences between the planned dose and the dose delivered using MLC tracking (49 fractions), gating (166 fractions), and no motion adaptation strategies (215 fractions) for individual fractions. The whiskers represent the minimum and maximum values. A star indicates a difference in mean between MLC tracking and gating where $p < 0.05$ and a diamond indicates a difference in variance where $p < 0.05$.

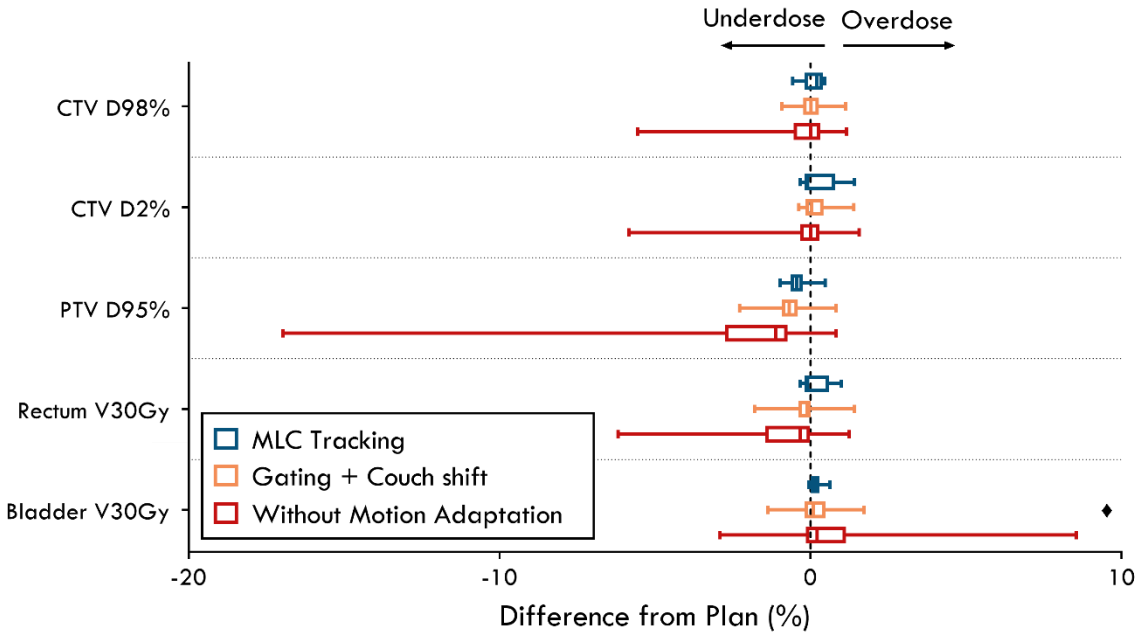

Figure 4. Patient doses. The differences between the planned dose and the dose delivered using MLC tracking (10 patients), gating (34 patients), and no motion adaptation strategies (44 patients) for the summed dose across five fractions. The whiskers represent the minimum and maximum values. A diamond indicates a difference between MLC tracking and gating in variance where $p < 0.05$.

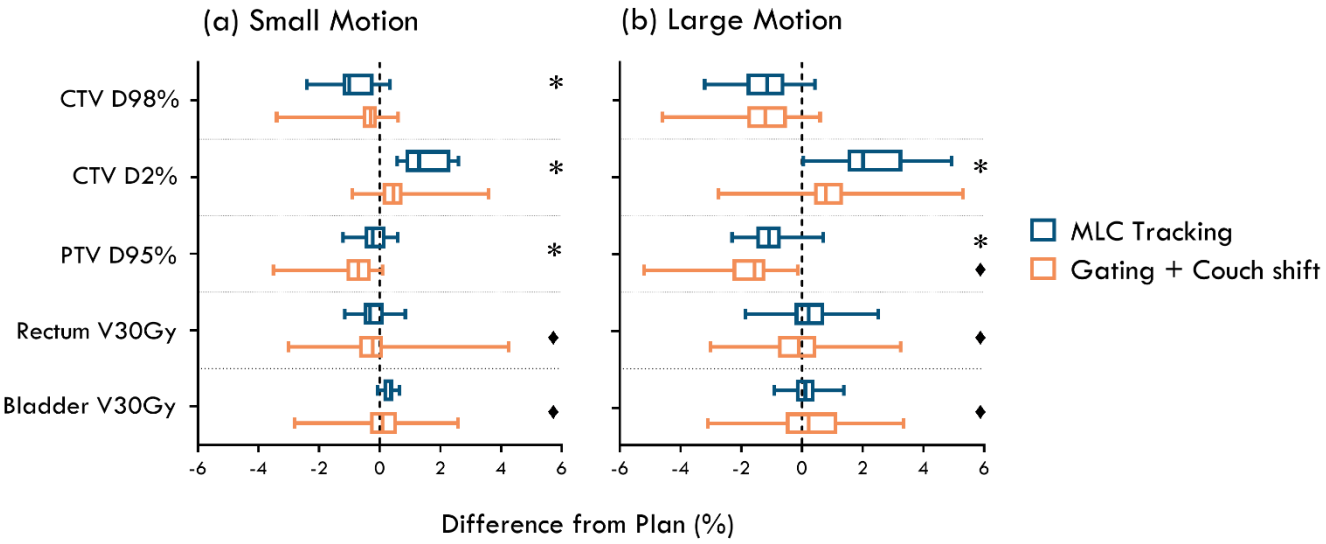

Figure 5. The difference between the planned dose and the dose delivered using MLC tracking and gating plotted for fractions with (a) small prostate motion (15 MLC tracking fractions and 100 gating fractions) and (b) large prostate motion (34 MLC tracking fractions and 65 gating fractions). Prostate motion was considered large if it exceeded the gating threshold of > 2mm for longer than 5 seconds. Whiskers represent the minimum and maximum values. A star indicates a difference in mean between MLC tracking and gating where $p < 0.05$ and a diamond indicates a difference in variance where $p < 0.05$.

The length of time required to perform each couch shift across the 65 gated fractions that required intervention is shown in Figure 6(a). The average time that was required to perform a couch shift was 3.5 ± 1.0 minutes. The total interruptions to treatment caused as a result of gating the beam and performing couch shifts is shown in Figure 6(b). On average 0.5 couch shifts were required per fraction and the average total interruption per fraction overall was 1.8 ± 2.6 minutes. The mean treatment time from the beginning of the CBCT to the end of the final treatment arc for the gating treatments was 10.6 ± 4.3 minutes.

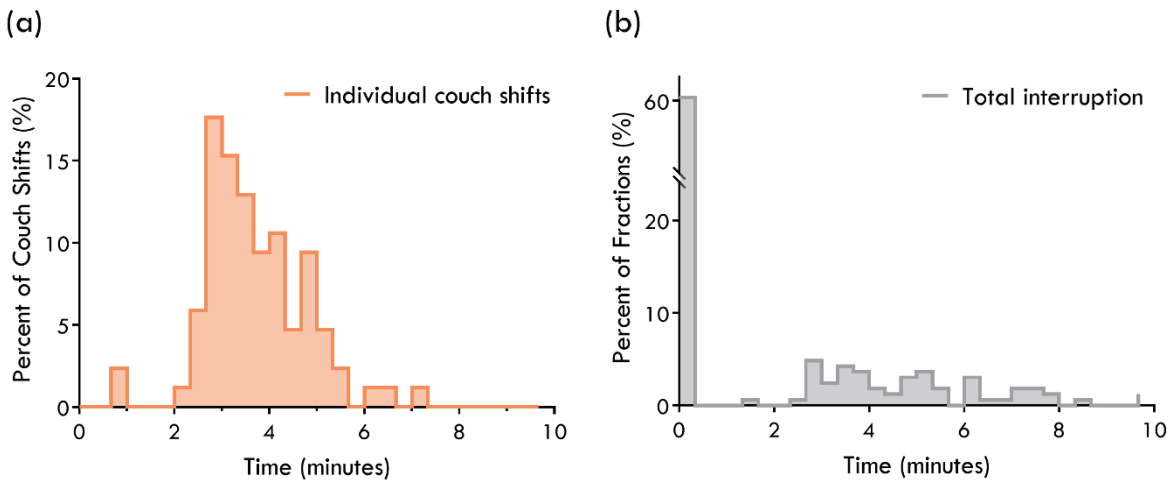

Figure 6. Histograms of (a) the time required to perform each couch shift and (b) the total interruption time occurring per fraction as a result of couch shifts.

Discussion

Reconstruction of the doses delivered using MLC tracking and gating in the TROG 15.01 SPARK trial, and treatments simulated with no motion adaptation, showed that both motion adaptation strategies were effective at improving the dose delivery accuracy. Figure 3 and Figure 4 showed that MLC tracking and gating resulted in doses that were more consistent with the original plan compared to treatment without motion adaptation.

A slightly larger distribution of prostate motion was seen for the MLC tracking fractions as shown in Figure 2. While this may be due to the lower patient numbers treated

with MLC tracking, this could also be attributed to differences in the treatment time. The beam-on times during MLC tracking treatment arcs were longer as patients were treated with a 6 MV beam (maximum dose rate 600MU/min), while the majority of gating patients were treated using 10 MV FFF (maximum dose rate 2400MU/min). However, the difference in the means and standard deviations of the observed motion between MLC tracking and gating were within 1 mm and were therefore unlikely to affect the dosimetric results.

The mean differences from the plan had little difference between MLC tracking and gating for the CTV $D_{98\%}$, PTV $D_{95\%}$, bladder $V_{30Gy,}$ and rectum V_{30Gy}. However, the range of differences from the plan was wider for gating for each of these dose metrics, and the variance of differences from the plan was larger than MLC tracking for the bladder and rectum. This suggests that while both motion adaptation strategies perform similarly on average, gating would result in doses that deviated more from the plan for the worst cases. Gating treatments also had a slightly higher correlation between the RMSE of the prostate displacement during treatment and the resulting dose difference from the plan for the CTV $D_{98\%}$, CTV $D_{2\%}$, PTV $D_{95\%}$, and bladder V_{30Gy} compared to MLC tracking, likely due to MLC tracking correcting for motion in real-time. The gating fraction that resulted in the largest overdose to the rectum V_{30Gy} of 4.3% had a mean 3D prostate displacement of 2.1 mm but never exceeded 2 mm in any direction for longer than 5 seconds to trigger intervention. Similarly, the gating fraction that resulted in the largest underdose to the PTV $D_{95\%}$ of -5.2% had a mean 3D prostate displacement of 2.2 mm that was not corrected. Gating also resulted in a larger dose discrepancy from the plan compared to the corresponding fraction simulated with no motion adaptation for four fractions (2.5% of fractions treated with gating), where the prostate would have had a smaller average displacement if a couch shift had not occurred, due to the prostate drifting back toward the set-up position after the intervention. Gating may instead show more dosimetric benefit when treating sites with larger magnitudes of motion.

Worm *et al.* [26] investigated the benefit of gating to manage respiratory-induced motion during liver SABR treatments compared to non-gated treatments and saw ranges of reduction in the CTV $D_{95\%}$ of 0.2% to 2.0% for gated fraction, compared to 0.7% to 22.0% for non-gated fractions.

MLC tracking has its own limitations. MLC tracking resulted in lower doses to the CTV $D_{98\%}$ and higher doses to the CTV $D_{2\%}$ for smaller prostate motions as shown in Figure 5. In a previous experimental study, Poulsen *et al*. [27] found that the main contributor to tracking error for prostate motion was leaf fitting errors that result from the finite MLC leaf width. The width of the MLC leaves used for MLC tracking in this study was 5 mm, so prostate motion perpendicular to the MLC leaves could only be corrected in intervals of 5 mm. To a lesser extent, the finite leaf speed also contributes to dosimetric errors. These errors resulted in colder and hotter spots for the CTV $D_{98\%}$ and CTV $D_{2\%}$ compared to gating, particularly for smaller prostate motions shown in Figure 5(a). These errors could be minimised by being detected and corrected for continuously throughout the treatment [28], which will be incorporated in future development.

MLC tracking can improve treatment efficiency compared to gating for motion adaptation. While 61% of fractions treated using gating did not have motion that required intervention, when intervention was required, gating the beam and repositioning the patient would result in considerable interruptions to treatment (3.5 ± 1.0 minutes per couch shift in our study). However, it should be noted that the duration of interruptions in Figure 6 were specific to this clinical trial and protocol used to perform couch shifts. All gating events were performed manually by the treatment team, and a kV-kV match was required to be performed before the couch could be repositioned [29], which contributed to the long interruption times in this study. These interruption times could be considerably reduced if KIM was fully integrated with the clinical system and allowed for automatic couch shifts.

Interruption frequency and duration may widely vary for different treatment sites that experience larger magnitudes of motion. For example, in the study by Worm *et al.* [26] the treatment times for liver patients treated in free-breathing using SABR were extended from 10 to 15 minutes for non-gated treatments, to a mean of 25.2 minutes for the gated treatments. Couch corrections were also performed to correct for baseline drift, with a mean of 2.8 couch corrections per fraction, resulting in more interruption compared to the prostate treatments in this study.

Treatment interruptions will also vary for different gating methods and thresholds. While patients in this study on average had 0.5 interventions per fraction, this was lower compared to the study by Lovelock *et al*. [14] which had 1.7 interventions per fraction for prostate patients. Treatments in Lovelock *et al*.'s study would be gated if prostate motion exceeded 2 mm for any amount of time, decreasing the efficiency of treatment compared to this trial where an intervention would only occur if prostate motion exceeded 2 or 3 mm for longer than 5 s. The 5 s threshold was chosen as a compromise between treatment efficiency and dosimetric accuracy, and to allow the treatment team to observe whether the prostate motion was transient such that a couch shift would not be beneficial. Treatment efficiency will decrease with stricter gating thresholds and should be carefully chosen to also balance the dosimetric accuracy.

Treatment interruptions should ideally be avoided for an efficient clinical workflow and minimise patient discomfort. Longer treatment times may also result in larger prostate displacements. Langen *et al*. [30] observed intrafraction prostate motion using electromagnetic tracking and found one-eighth of their observations after 5 min showed displacements larger than 3 mm, however this increased to one-quarter of observations made after 10 min. Steiner *et al*. [31] evaluated prostate motion for patients with endorectal balloons inserted and found that the mean prostate displacement increased with treatment

time, requiring larger margins for longer treatments. However, we did not observe any decreases in prostate motion for MLC tracking fractions in this study due to other differing treatment factors between treatment centres that affected treatment time.

The accuracy of each adaptation method will be limited by the accuracy of the tumour localization method. In this study, all adaptation processes were performed according to motion information output by KIM. The 3D tumour localization accuracy of KIM in the TROG 15.01 SPARK trial was quantified to be 0.0 ± 0.5, 0.0 ± 0.4 and 0.1 ± 0.3 mm in AP, LR and SI directions respectively [23]. Other target localization methods such as the Calypso system have previously been used to guide SABR treatments for various anatomical sites [14, 19, 26, 32]. The accuracy of Calypso is comparable to KIM, with sub-millimetre localization accuracy and precision [33, 34]. Calypso is clinically approved and can provide motion guidance without the need for additional imaging dose, or any pauses in position information. Meanwhile, KIM provides real-time tumour position in 6 degrees-of-freedom using fiducial markers that are MR-compatible and smaller than the beacons used with Calypso. KIM also offers a solution that is highly accessible in comparison to specialised systems such as Calypso, as it utilizes the on-board kV imager that is already equipped on modern linacs, potentially allowing widespread implementation of SABR.

Specialised systems such as the CyberKnife have also been extensively implemented for SABR prostate treatments with promising results [35]. Colvill *et al.* [36] performed an experimental comparison of various real-time adaptive radiotherapy techniques, including the use of the CyberKnife and MLC tracking for lung and prostate SABR treatments. Each real-time motion adaptation technique performed similarly for both the lung and prostate, suggesting that MLC tracking could provide an accessible alternative to CyberKnife. While dosimetric differences were not observed, there was a considerable difference in treatment

times, with a mean of 37 minutes for CyberKnife treatment and 4.5 minutes for MLC tracking treatment.

A limitation of this study was that this was not a randomised trial and there was an imbalance in the patient numbers (10 patients for MLC tracking and 44 for gating). While treatments were standardised to adhere to a trial protocol [20] it is possible that other uncontrolled factors may influence the results. This study was also limited by the dose reconstruction method, as the effect of target rotations and deformations on the dose could not be calculated. The intrafraction deformation of organs was not known during treatment so the dose to the prostate as well as the V_{30Gy} for the bladder and rectum were both calculated based on volumes from the planning CT. Despite this, deformations of the rectum due to filling are the main contributions to prostate motion and causes the prostate to deform [37], resulting in uncertainty for our calculated doses.

MLC tracking and gating were also both limited in that they did not account for rotations and deformations in this study. However, Wolf *et al*. [38] found that the dosimetric impact of rotations were minimal. MLC tracking was also limited by static jaws which had to be widened to allow for MLC tracking. An additional 8 mm was added to the field size in each direction, however if target motion exceeded this expansion the beam would be gated and the patient repositioned, which occurred in three fractions. This limitation could potentially be reduced by implementing a dynamic jaw. A couch shift was also used in eight MLC tracking fractions where prostate displacement perpendicular to the MLC leaves persisted at approximately half a leaf width (i.e. 2.5 mm), to compensate for dosimetric inaccuracies that could result from leaf fitting errors.

Future work could address the limitations with gating by clinically implementing real-time couch tracking [39] to allow for motion corrections that do not have an impact on the

efficiency of treatment. Studies have found better agreement with the planned dose and dose delivered to moving phantoms using couch tracking compared to MLC tracking [40-42]. Couch tracking can improve on tracking accuracy for motion perpendicular to the MLC leaves and is not restricted by the plan modulation. Ehrbar *et al.* [42] compared couch tracking and MLC tracking for SABR prostate cancer plans and found an increase in dose to the target structures using MLC tracking compared to a static measurement. This is similar to what was seen in this trial, with higher CTV $D_{98\%}$ and CTV $D_{2\%}$ delivered using MLC tracking compared to gating. Ehrbar *et al.* also saw an increase to the urethra Dmax. The hotspots seen during MLC tracking in this trial may similarly degrade the urethra dose, however the locations of these hotspots are random so their impact will be minimised when summing all fractions. MLC tracking does, however, have advantages over couch corrections including the potential to correct for rotations [43], deformations [44] and multiple targets [44, 45]. Ideal real-time motion adaptation may instead be achieved by integrating MLC and couch tracking [46].

In this study, the dosimetric efficacy of two intrafraction adaptation strategies, MLC tracking and gating, was evaluated using a standard linac to treat SABR patients in a prospective clinical trial. Both MLC tracking and gating were similarly effective at delivering a dose closer to the treatment plan compared to when no motion adaptation strategy is used. While on average both motion adaptation strategies had comparable differences from the planned doses, gating had a larger variance from the original plan for the OARs in this study With the low barrier to implementation on a standard linac system for these motion adaptation strategies, both MLC tracking and gating could provide a low-cost option for intrafraction motion adaptation and make SABR treatments accessible to a wider range of patients.

References

1. King, C.R., D. Freeman, I. Kaplan, D. Fuller, G. Bolzicco, S. Collins, et al., *Stereotactic body radiotherapy for localized prostate cancer: Pooled analysis from a multi-institutional consortium of prospective phase II trials.* Radiotherapy and Oncology, 2013. **109**(2): p. 217-221.
2. Katz, A.J. and J. Kang, *Stereotactic Body Radiotherapy as Treatment for Organ Confined Low- and Intermediate-Risk Prostate Carcinoma, a 7-Year Study.* Frontiers in Oncology, 2014. **4**(240).
3. King, C.R., S. Collins, D. Fuller, P.-C. Wang, P. Kupelian, M. Steinberg, et al., *Health-related quality of life after stereotactic body radiation therapy for localized prostate cancer: results from a multi-institutional consortium of prospective trials.* International Journal of Radiation Oncology* Biology* Physics, 2013. **87**(5): p. 939-945.
4. Kishan, A.U., A. Dang, A.J. Katz, C.A. Mantz, S.P. Collins, N. Aghdam, et al., *Long-term outcomes of stereotactic body radiotherapy for low-risk and intermediate-risk prostate cancer.* JAMA network open, 2019. **2**(2): p. e188006-e188006.
5. Widmark, A., A. Gunnlaugsson, L. Beckman, C. Thellenberg-Karlsson, M. Hoyer, M. Lagerlund, et al., *Ultra-hypofractionated versus conventionally fractionated radiotherapy for prostate cancer: 5-year outcomes of the HYPO-RT-PC randomised, non-inferiority, phase 3 trial.* The Lancet, 2019. **394**(10196): p. 385-395.
6. Morgan, S.C., K. Hoffman, D.A. Loblaw, M.K. Buyyounouski, C. Patton, D. Barocas, et al., *Hypofractionated radiation therapy for localized prostate cancer: An ASTRO, ASCO, and AUA evidence-based guideline.* The Journal of urology, 2018.
7. Pan, H., D.R. Simpson, L.K. Mell, A.J. Mundt, and J.D. Lawson, *A survey of stereotactic body radiotherapy use in the United States.* Cancer, 2011. **117**(19): p. 4566-4572.
8. Buyyounouski, M.K., R.A. Price, E.E. Harris, R. Miller, W. Tomé, T. Schefter, et al., *Stereotactic body radiotherapy for primary management of early-stage, low-to intermediate-risk prostate cancer: report of the American Society for Therapeutic Radiology and Oncology Emerging Technology Committee.* International Journal of Radiation Oncology• Biology• Physics, 2010. **76**(5): p. 1297-1304.
9. Martin, J., P. Keall, S. Siva, P. Greer, D. Christie, K. Moore, et al., *TROG 18.01 phase III randomised clinical trial of the Novel Integration of New prostate radiation schedules with adJuvant Androgen deprivation: NINJA study protocol.* BMJ open, 2019. **9**(8): p. e030731.
10. Schweikard, A., H. Shiomi, and J. Adler, *Respiration tracking in radiosurgery.* Medical Physics, 2004. **31**(10): p. 2738-2741.
11. Schnarr, E., M. Beneke, D. Casey, E. Chao, J. Chappelow, A. Cox, et al., *Feasibility of real-time motion management with helical tomotherapy.* Medical Physics, 2018. **45**(4): p. 1329-1337.
12. Takayama, K., T. Mizowaki, M. Kokubo, N. Kawada, H. Nakayama, Y. Narita, et al., *Initial validations for pursuing irradiation using a gimbals tracking system.* Radiotherapy and Oncology, 2009. **93**(1): p. 45-49.
13. Korreman, S.S., *Motion in radiotherapy: photon therapy.* Physics in Medicine and Biology, 2012. **57**(23): p. R161-R191.
14. Lovelock, D.M., A.P. Messineo, B.W. Cox, M.A. Kollmeier, and M.J. Zelefsky, *Continuous monitoring and intrafraction target position correction during treatment improves target coverage for patients undergoing SBRT prostate therapy.*

International Journal of Radiation Oncology* Biology* Physics, 2015. **91**(3): p. 588-594.
15. Keall, P.J., J.A. Ng, P. Juneja, R.T. O'Brien, C.-Y. Huang, E. Colvill, et al., *Real-Time 3D Image Guidance Using a Standard LINAC: Measured Motion, Accuracy, and Precision of the First Prospective Clinical Trial of Kilovoltage Intrafraction Monitoring–Guided Gating for Prostate Cancer Radiation Therapy.* International Journal of Radiation Oncology*Biology*Physics, 2016. **94**(5): p. 1015-1021.
16. Keall, P.J., E. Colvill, R. O' Brien, J.A. Ng, P.R. Poulsen, T. Eade, et al., *The first clinical implementation of electromagnetic transponder‐guided MLC tracking.* Medical physics, 2014. **41**(2).
17. Colvill, E., J.T. Booth, R.T. O'Brien, T.N. Eade, A.B. Kneebone, P.R. Poulsen, et al., *Multileaf Collimator Tracking Improves Dose Delivery for Prostate Cancer Radiation Therapy: Results of the First Clinical Trial.* International Journal of Radiation Oncology*Biology*Physics, 2015. **92**(5): p. 1141-1147.
18. Keall, P.J., D.T. Nguyen, R. O'Brien, V. Caillet, E. Hewson, P.R. Poulsen, et al., *The first clinical implementation of real-time image-guided adaptive radiotherapy using a standard linear accelerator.* Radiotherapy and Oncology, 2018. **127**(1): p. 6-11.
19. Booth, J.T., V. Caillet, N. Hardcastle, R. O'Brien, K. Szymura, C. Crasta, et al., *The first patient treatment of electromagnetic-guided real time adaptive radiotherapy using MLC tracking for lung SABR.* Radiotherapy and Oncology, 2016. **121**(1): p. 19-25.
20. Keall, P., D.T. Nguyen, R. O'Brien, J. Booth, P. Greer, P. Poulsen, et al., *Stereotactic prostate adaptive radiotherapy utilising kilovoltage intrafraction monitoring: the TROG 15.01 SPARK trial.* BMC cancer, 2017. **17**(1): p. 180.
21. Poulsen, P.R., B. Cho, K. Langen, P. Kupelian, and P.J. Keall, *Three-dimensional prostate position estimation with a single x-ray imager utilizing the spatial probability density.* Physics in Medicine & Biology, 2008. **53**(16): p. 4331.
22. Tehrani, J.N., R.T. O'Brien, P.R. Poulsen, and P. Keall, *Real-time estimation of prostate tumor rotation and translation with a kV imaging system based on an iterative closest point algorithm.* Physics in Medicine and Biology, 2013. **58**(23): p. 8517-8533.
23. Hewson, E.A., D.T. Nguyen, R. O'Brien, J.H. Kim, T. Montanaro, T. Moodie, et al., *The accuracy and precision of the KIM motion monitoring system used in the multi‐institutional TROG 15.01 Stereotactic Prostate Ablative Radiotherapy with KIM (SPARK) trial.* Medical physics, 2019. **46**(11): p. 4725-4737.
24. Keall, P., D.T. Nguyen, R. O'Brien, E. Hewson, H. Ball, P. Poulsen, et al., *Real-Time Image-Guided Ablative Prostate Cancer Radiation Therapy: Results from the TROG 15.01 SPARK Trial.* International Journal of Radiation Oncology* Biology* Physics, 2020.
25. Poulsen, P.R., M.L. Schmidt, P. Keall, E.S. Worm, W. Fledelius, and L. Hoffmann, *A method of dose reconstruction for moving targets compatible with dynamic treatments.* Medical Physics, 2012. **39**(10): p. 6237-6246.
26. Worm, E.S., M. Høyer, R. Hansen, L.P. Larsen, B. Weber, C. Grau, et al., *A prospective cohort study of gated stereotactic liver radiation therapy using continuous internal electromagnetic motion monitoring.* International Journal of Radiation Oncology* Biology* Physics, 2018. **101**(2): p. 366-375.
27. Poulsen, P.R., W. Fledelius, B. Cho, and P. Keall, *Image-based dynamic multileaf collimator tracking of moving targets during intensity-modulated arc therapy.* International Journal of Radiation Oncology* Biology* Physics, 2012. **83**(2): p. e265-e271.

28. Wisotzky, E., R. O'Brien, and P.J. Keall, *A novel leaf sequencing optimization algorithm which considers previous underdose and overdose events for MLC tracking radiotherapy.* Medical physics, 2016. **43**(1): p. 132-136.
29. Nguyen, D.T., R. O'Brien, J.-H. Kim, C.-Y. Huang, L. Wilton, P. Greer, et al., *The first clinical implementation of a real-time six degree of freedom target tracking system during radiation therapy based on Kilovoltage Intrafraction Monitoring (KIM).* Radiotherapy and Oncology, 2017. **123**(1): p. 37-42.
30. Langen, K.M., T.R. Willoughby, S.L. Meeks, A. Santhanam, A. Cunningham, L. Levine, et al., *Observations on Real-Time Prostate Gland Motion Using Electromagnetic Tracking.* International Journal of Radiation Oncology*Biology*Physics, 2008. **71**(4): p. 1084-1090.
31. Steiner, E., D. Georg, G. Goldner, and M. Stock, *Prostate and Patient Intrafraction Motion: Impact on Treatment Time-Dependent Planning Margins for Patients With Endorectal Balloon.* International Journal of Radiation Oncology*Biology*Physics, 2013. **86**(4): p. 755-761.
32. Mantz, C., E. Fernandez, I. Zucker, and S. Harrison, *A phase II trial of real-time target tracking SBRT for low-risk prostate cancer utilizing the Calypso 4D localization system: patient reported health-related quality of life and toxicity outcomes.* International Journal of Radiation Oncology• Biology• Physics, 2010. **78**(3): p. S57-S58.
33. Willoughby, T.R., P.A. Kupelian, J. Pouliot, K. Shinohara, M. Aubin, M. Roach III, et al., *Target localization and real-time tracking using the Calypso 4D localization system in patients with localized prostate cancer.* International Journal of Radiation Oncology* Biology* Physics, 2006. **65**(2): p. 528-534.
34. Franz, A., D. Schmitt, A. Seitel, M. Chatrasingh, G. Echner, U. Oelfke, et al., *Standardized accuracy assessment of the calypso wireless transponder tracking system.* Physics in Medicine & Biology, 2014. **59**(22): p. 6797.
35. Katz, A.J., *CyberKnife radiosurgery for prostate cancer.* Technology in cancer research & treatment, 2010. **9**(5): p. 463-472.
36. Colvill, E., J. Booth, S. Nill, M. Fast, J. Bedford, U. Oelfke, et al., *A dosimetric comparison of real-time adaptive and non-adaptive radiotherapy: a multi-institutional study encompassing robotic, gimbaled, multileaf collimator and couch tracking.* Radiotherapy and Oncology, 2016. **119**(1): p. 159-165.
37. Ghadjar, P., C. Fiorino, P.M. af Rosenschöld, M. Pinkawa, T. Zilli, and U.A. van Der Heide, *ESTRO ACROP consensus guideline on the use of image guided radiation therapy for localized prostate cancer.* Radiotherapy and Oncology, 2019. **141**: p. 5-13.
38. Wolf, J., J. Nicholls, P. Hunter, D.T. Nguyen, P. Keall, and J. Martin, *Dosimetric impact of intrafraction rotations in stereotactic prostate radiotherapy: A subset analysis of the TROG 15.01 SPARK trial.* Radiotherapy and Oncology, 2019. **136**: p. 143-147.
39. D'Souza, W.D., S.A. Naqvi, and C.X. Yu, *Real-time intra-fraction-motion tracking using the treatment couch: a feasibility study.* Physics in Medicine and Biology, 2005. **50**(17): p. 4021-4033.
40. Menten, M.J., M. Guckenberger, C. Herrmann, A. Krauß, S. Nill, U. Oelfke, et al., *Comparison of a multileaf collimator tracking system and a robotic treatment couch tracking system for organ motion compensation during radiotherapy.* Medical Physics, 2012. **39**(11): p. 7032-7041.

41. Hansen, R., T. Ravkilde, E.S. Worm, J. Toftegaard, C. Grau, K. Macek, et al., *Electromagnetic guided couch and multileaf collimator tracking on a TrueBeam accelerator.* Medical physics, 2016. **43**(5): p. 2387-2398.
42. Ehrbar, S., S. Schmid, A. Jöhl, S. Klöck, M. Guckenberger, O. Riesterer, et al., *Comparison of multi-leaf collimator tracking and treatment-couch tracking during stereotactic body radiation therapy of prostate cancer.* Radiotherapy and Oncology, 2017. **125**(3): p. 445-452.
43. Wu, J., D. Ruan, B. Cho, A. Sawant, J. Petersen, L.J. Newell, et al., *Electromagnetic Detection and Real-Time DMLC Adaptation to Target Rotation During Radiotherapy.* International Journal of Radiation Oncology*Biology*Physics, 2012. **82**(3): p. e545-e553.
44. Ge, Y., R.T. O’ Brien, C.C. Shieh, J.T. Booth, and P.J. Keall, *Toward the development of intrafraction tumor deformation tracking using a dynamic multi‐leaf collimator.* Medical physics, 2014. **41**(6Part1): p. 061703.
45. Ludlum, E., G. Mu, V. Weinberg, M. Roach III, L.J. Verhey, and P. Xia, *An algorithm for shifting MLC shapes to adjust for daily prostate movement during concurrent treatment with pelvic lymph nodesa).* Medical Physics, 2007. **34**(12): p. 4750-4756.
46. Toftegaard, J., R. Hansen, T. Ravkilde, K. Macek, and P.R. Poulsen, *An experimentally validated couch and MLC tracking simulator used to investigate hybrid couch-MLC tracking.* Medical Physics, 2017. **44**(3): p. 798-809.